Anti-adherent biomaterials for prevention of catheter biofouling

McCoy, C. P., Irwin, N. J., Donnelly, L., Jones, D. S., Hardy, J. G., & Carson, L. (2018). Anti-adherent biomaterials for prevention of catheter biofouling. *International Journal of Pharmaceutics*, *535*(1-2), 420-427. https://doi.org/10.1016/j.ijpharm.2017.11.043

Published in:
International Journal of Pharmaceutics

Document Version:
Peer reviewed version

Queen's University Belfast - Research Portal:
Link to publication record in Queen's University Belfast Research Portal

Anti-Adherent Biomaterials for Prevention of Catheter Biofouling

Colin P. McCoy*, Nicola J. Irwin, Louise Donnelly, David S. Jones, John G. Hardy, Louise Carson

School of Pharmacy, Queen's University Belfast, 97 Lisburn Road, Belfast BT9 7BL, Northern Ireland, UK.

*To whom correspondence should be addressed. (Tel: +44 28 9097 2081; Fax: +44 28 9024 7794; e-mail: c.mccoy@qub.ac.uk)

Abstract

Medical device-associated infections present a leading global healthcare challenge, and effective strategies to prevent infections are urgently required. Herein, we present an innovative anti-adherent hydrogel copolymer as a candidate catheter coating with complementary hydrophobic drug-carrying and eluting capacities. The amphiphilic block copolymer, Poloxamer 188, was chemically-derivatized with methacryloyl moieties and copolymerized with the hydrogel monomer, 2-hydroxyethyl methacrylate. Performance of the synthesized copolymers was evaluated in terms of equilibrium swelling, surface water wettability, mechanical integrity, resistance to encrustation and bacterial adherence, and ability to control release of the loaded fluoroquinolone antibiotic, ofloxacin. The developed matrices were able to provide significant protection from fouling, with observed reductions of over 90% in both adherence of the common urinary pathogen *Escherichia coli* and encrusting crystalline deposits of calcium and magnesium salts relative to the commonly employed hydrogel, poly(hydroxyethyl methacrylate). Additionally, the

release kinetics of a loaded hydrophobic drug could be readily tuned through facile manipulation of polymer composition. This combinatorial approach shows significant promise in the development of suitable systems for prevention of catheter-associated infections.

Keywords

Hydrophobic drug release; biofouling; Poloxamer; encrustation

1. Introduction

Implanted medical devices are of increasing importance within current clinical applications (Gilmore and Carson 2015). The susceptibility of such implants to infection, however, represents a global healthcare challenge with associated patient morbidity and potentially fatal outcomes (Cloutier, et al. 2015; Francolini, et al. 2014). In this regard, bacterial colonization of urinary catheters, which are inserted in up to one quarter of hospitalized patients to drain urine from their bladders (Daniels, et al. 2014), represents a particular concern. Catheter-associated urinary tract infections (CAUTIs) are responsible for 40% of all nosocomial infections and in excess of 100,000 hospital admissions in the US per annum (Fisher, et al. 2015). Furthermore, the burden of CAUTIs from a financial perspective has increased significantly on account of the recent decision by the US Centers for Medicare and Medicaid Services to cease funding treatment of these 'reasonably preventable' nosocomial infections (Greene, et al. 2014).

Multiplication of adherent organisms with subsequent biofilm formation and seeding

of the bladder mucosa and urine by planktonic bacteria make treatment of medical device-associated infections particularly challenging (Daniels, et al. 2014). Much research is now directed towards the development of preventative strategies, such as anti-fouling device coatings, to prevent bacterial attachment (Cloutier, et al. 2015). Antimicrobial-eluting coatings based on antibiotics, metals or antiseptics, such as gentamicin, silver and gendine respectively, have been the subject of significant research (Cloutier, et al. 2015; Jamal, et al. 2015; Wang, et al. 2015). To-date, however, issues surrounding the emergence of resistant microorganisms, potential selection of non-sensitive strains, toxicity to host cells and the limited antibacterial loading capacity of surface coatings have restricted their widespread clinical employment (Cloutier, et al. 2015; Coad, et al. 2016).

Alternatively, non-release-based approaches, such as surface functionalization with hydrophilic polymers such as polyethylene glycol, have demonstrated promising antifouling ability *in vitro* (Wei, et al. 2014). The presence of a tightly-bound water layer on the polymer surface in combination with dynamic movement of the outward-projecting polymer chains effectively hinder attachment of bacterial cells by acting as physical and steric barriers (Francolini, et al. 2014; Gultekinoglu, et al. 2015; Rodriguez-Emmenegger, et al. 2015). Their efficacy in resisting bacterial colonization and ultimate biofilm development *in vivo,* however, is ultimately compromized by the non-specific and rapid coverage of the device surface with a layer of proteins and other cellular matter (Cloutier, et al. 2015).

The aim of this study was to provide a novel and effective approach for optimizing the anti-fouling ability of a passive anti-adherent hydrophilic polymer surface, as a candidate coating for infection-resistant medical devices, namely through pairing with active agent release to provide a “belt and braces” dual approach to disfavor biofilm

establishment. The effect of chemical modification with an amphiphilic block copolymer, Poloxamer 188, on surface water wettability, swellability, tensile properties, encrustation and bacterial resistance of the biocompatible hydrogel, poly(hydroxyethyl methacrylate) (p(HEMA)), was first of all investigated. This was subsequently followed by examination of the capacity of the candidate device coating materials synthesized herein for incorporation and subsequent release of the broad-spectrum fluoroquinolone antibiotic, ofloxacin.

2. Materials and methods

2.1. Materials

All materials were of analytical grade or higher and were used as supplied. 2,2'-Azobisisobutyronitrile (AIBN) was obtained from Acros Organics (Leicestershire, UK). Methacryloyl chloride, dichloromethane (DCM), triethylamine, 2-hydroxyethyl methacrylate (2-HEMA), benzalkonium chloride, ofloxacin and urease (Type IX; Jack Bean) were purchased from Aldrich (Dorset, UK). Poloxamer 188 (Lutrol® F68) was obtained from BASF (Ludwigshafen, Germany). Pyridine, magnesium chloride hexahydrate, calcium chloride hexahydrate, potassium dihydrogen orthophosphate and urea were obtained from BDH Laboratories (Dorset, UK). Mueller-Hinton agar and Mueller-Hinton broth were purchased from Oxoid (Basingstoke, UK).

2.2. Methods

Poloxamers are a series of amphiphilic, non-ionic block copolymers with a central hydrophobic poly(propylene oxide) (PPO) segment flanked by two poly(ethylene oxide) (PEO) chains (Kaizu and Alexandridis 2015). When in solution at

concentrations above a critical micelle concentration, the molecules aggregate in a process driven by hydrophobic interactions of the PPO blocks (Li and Zhang 2016). The inner hydrophobic PPO cores of the resulting micellar structures have been exploited for the loading and release of hydrophobic drugs (Li, et al. 2015), and the shielding of toxic drugs until their release at targeted tissue sites (Movassaghian, et al. 2015). In addition to their high solubilizing capacity and low toxicity, the conformational flexibility of the outer hydrophilic corona of PEO chains functions to repel approaching bacteria and other particulate matter from the surface (Zeng, et al. 2014). In this study, we first of all functionalized Poloxamer 188 molecules with methacryloyl moieties to yield polymerisable derivatives for copolymerisation with the hydrogel monomer, 2-HEMA. By controlling the stoichiometric mass of methacryloyl chloride added to the reaction mixture, poloxamer moieties could be modified at one terminal hydroxyl group (monomethacrylation) or at both terminal hydroxyl positions (dimethacrylation) to additionally facilitate functioning of the poloxamer derivative as a crosslinker.

2.2.1. Synthesis of mono- and dimethacrylated Poloxamer 188 (MMP and DMP)

Components were added to a glass round-bottomed flask in the amounts stated in Table 1 according to the following procedure. Poloxamer 188 was dissolved in DCM (275 mL for monomethacrylation; 175mL for dimethacrylation) and triethylamine. After cooling to 0°C over an ice bath, a solution of methacryloyl chloride in DCM (25 mL for monomethacrylation; 40 mL for dimethacrylation) was added dropwise with stirring. The ice bath was then removed and the solution stirred for a further 24 h before filtration, evaporation of the solvent and washing with deionized water to yield a white solid.

Table 1: Component masses (g, mmoL) employed for mono- and dimethacrylation of Poloxamer 188

Chemical	Mass for monomethacrylation (g, mmoL)	Mass for dimethacrylation (g, mmoL)
Poloxamer 188	67.3, 7.8	42.07, 4.89
Triethylamine	0.14, 1.01	1.4, 10.06
Methacryloyl chloride	0.1, 1.03	0.95, 9.78

Following synthesis, elucidation of monomer structure was performed using FTIR spectroscopy. Samples were prepared as KBr discs, and spectra recorded on a Jasco FTIR-4100 spectrometer between 4000 and 400 cm^{-1}. Success of the reaction was confirmed by the presence of a new band at 1717 cm^{-1} in spectra of the MMP and DMP reaction products, attributed to the newly formed carbonyl ester moiety.

2.2.2. Preparation of poly(monomethacrylated poloxamer-*co*-hydroxyethyl methacrylate) (p(MMP-*co*-HEMA)) copolymers

P(MMP-*co*-HEMA) copolymers containing MMP in weight ratios of 1%, 5% and 10% relative to the content of HEMA were prepared by the respective addition of 0.755 g, 3.775 g and 7.55g of the MMP reaction product (comprising 0.1 g, 0.5 g and 1.0 g of MMP, respectively, and unreacted Poloxamer 188) to 2-HEMA (10 g) and AIBN (0.05 g) with stirring. Following dissolution, mixtures were injected into moulds comprising two vertical glass plates lined with release liner, separated by silicone tubing and clamped together by bulldog clips. The polymers were cured at

60°C for 18 h, then soaked in successive volumes of deionized water to remove unreacted poloxamer. The amount of poloxamer leaching from the films was determined as a function of time by evaporation of the MMP-HEMA rinsing solutions and, when no further poloxamer leached from the synthesized films, polymers were stored in their hydrated state prior to testing.

2.2.3. Preparation of poly(dimethacrylated poloxamer-*co*-hydroxyethyl methacrylate) (p(DMP-*co*-HEMA)) copolymers

P(DMP-*co*-HEMA) copolymers containing DMP in weight ratios of 1%, 5% and 10% relative to the content of HEMA were prepared by the respective addition of 0.1 g, 0.5 g and 1.0 g DMP to 2-HEMA (10 g) and AIBN (0.05 g) with stirring. Following dissolution, mixtures were injected into moulds, as described for the p(MMP-*co*-HEMA) copolymers, and cured at 60°C for 18 h. Copolymers were then washed in successive volumes of deionized water over a 48 h period and stored in their hydrated state until testing.

2.2.4. Preparation of poly(hydroxyethyl methacrylate) (p(HEMA)) control

A control p(HEMA) polymer was prepared by mixing 2-HEMA (10 g) and AIBN (0.05 g) with stirring, injecting into moulds and curing at 60°C, as described for the copolymers. Again, the polymers were washed with successive volumes of water over a 48 h period and stored in their hydrated state until testing.

2.2.5. Preparation of non-methacrylated poloxamer-loaded poly(hydroxyethyl methacrylate) ((NMP-loaded p(HEMA))

P(HEMA) polymers loaded with non-methacrylated poloxamer (NMP) in a mass

approximating the mass of unreacted poloxamer remaining within 5% p(MMP-*co*-HEMA) copolymers after the rinsing step were prepared by dissolving Poloxamer 188 (3.275 g) and AIBN (0.05 g) in 2-HEMA (10 g). Solutions were injected into glass plate moulds and following polymerization, the films were washed as previously described.

2.2.6. Polymer characterisation

2.2.6.1. Equilibrium water content

Swollen polymer samples (2 cm x 1 cm) were dried at room temperature and residual water subsequently removed by freeze-drying (Modulyo freeze dryer F101-01-000). Samples were weighed, immersed in deionized water, and then reweighed at hourly intervals, following removal of excess surface water with a lens tissue, until a constant mass was achieved. The equilibrium water content (EWC), defined as the ratio of the mass of water in the hydrated sample to the dry sample mass, was calculated according to the following equation:

EWC (%) = (Hydrated sample mass – Dry sample mass)/Dry sample mass x 100

2.2.6.2. Contact angle analysis

Advancing and receding dynamic contact angles of all synthesized polymers were determined by the Wilhelmy plate technique using a Dynamic Contact Angle Analyser (DCA 312, Cahn Instruments), as previously described (Jones, et al. 2002). Briefly, samples (3 cm x 1 cm) were attached to a microbalance and immersed into, and withdrawn from, HPLC-grade water at a rate of 150 μms^{-1}. The wetting force at the solid/liquid/vapour interface was automatically recorded as a function of

immersion depth and time by a Cahn electrobalance and converted into advancing and receding contact angles by the instrument software.

2.2.6.3. Tensile analysis

Tensile analysis of the synthesized polymers was performed using a Stable Micro Systems TA-XT2 Texture Analyser (Goldaming, Surrey, UK), as previously described (Jones, et al. 2002). Hydrated dumbbell-shaped polymer samples (6 cm x 1 cm) were fixed between lower (static) and upper (moveable) clamps, spaced at a distance of 5 cm. The upper clamp was vertically raised at a constant crosshead speed of 0.5 mms^{-1} until fracture of the film occurred. Ultimate tensile strength and Young's modulus were calculated from the resultant plot of stress versus strain using the following equations:

Ultimate tensile strength (Pa) = Force at break (N)/Cross-sectional area (m^2)

Young's modulus = Tensile stress (Pa)/Strain

2.2.6.4. Calcium and magnesium encrustation

Polymer discs (8 mm diameter) were mounted onto needles secured to the lid of a plastic vessel (1 L) containing artificial urine with a similar composition to that employed by Tunney *et al.* (1996), but with a reduced concentration of albumin (Tunney, et al. 1996). Solutions A (450 mL), B (450 mL) and C (57 mL), the compositions and storage conditions of which are shown in Table 2, were added to the reaction vessel separately to prevent precipitation of brushite ($CaHPO_4.2H_2O$).

Table 2: Composition of artificial urine

Solution	Component	(% w/v)	Storage conditions
A	Potassium dihydrogen orthophosphate	0.76	Room temperature
	Magnesium chloride hexahydrate	0.36	
	Urea	1.0	
B	Calcium chloride hexahydrate	0.53	4°C
	Chicken ovalbumin	0.04	
C	Jack bean urease (Type IX)	0.125	4°C

The vessel was shaken in an orbital incubator (100 rpm, 37°C) to simulate conditions in the bladder, and artificial urine solution (140 mL) was replaced daily with fresh media. After one week, polymer samples were immersed in acetic acid (8 mL, 1 M) and sonicated for 4 h to dissolve the encrusted deposits, as previously described (Tunney and Gorman 2002). The resulting solutions were filtered to remove trace albumin and the quantities of calcium and magnesium present on each sample determined by atomic absorption spectrophotometry following calibration with standard solutions. Results are displayed as encrustation surface densities ($\mu g.cm^{-2}$).

2.2.6.5. Microbiological assessment

Clinical isolates of *Escherichia coli* were obtained from microbial biofilm present on retrieved ureteral stents and maintained on Müeller-Hinton agar slopes at 4°C (Keane et al. 1994). Subculturing was performed at three-monthly intervals. When required for the bacterial adherence assay, stationary phase *E. coli* was cultured by inoculating into Müeller-Hinton broth and incubating at 37°C in an orbital incubator (100 rpm) for 18 h. The culture was then centrifuged at 3000 *g* for 10 min and, after discarding the supernatant, the resulting pellet was resuspended in sterile peptone water (0.9%) to an optical density equivalent to approximately 1 x 10^8 cfumL^{-1}. Polymer discs (8 mm diameter) mounted on needles attached to lids of glass McCartney bottles were immersed in bacterial suspensions (20 mL) and shaken in an orbital incubator at 37°C for 4 h. Following incubation, non-adherent bacteria were removed by successively washing the samples with sterile peptone water (3 x 5 mL). Individual samples were then immersed in peptone water (10 mL), sonicated in an ultrasonic bath for 5 min and vortexed for 30 sec to remove adherent bacteria. Viable counts were determined by the Miles and Misra drop technique on Müeller-Hinton agar and plates were incubated overnight at 37°C (Miles, et al. 1938).

2.2.6.6. Drug loading and release

Drug loading was achieved *via* the equilibrium partitioning technique. Polymer samples suspended on hypodermic needles were immersed for 24 h in aqueous benzalkonium chloride solutions (1% w/v) saturated with ofloxacin. Polymer-bearing needles were removed from the drug loading solutions, suspended in pre-heated buffer solutions of aqueous benzalkonium chloride (1% w/v) and shaken in an orbital incubator at 37°C (100rpm). After designated time intervals, the needles were

transferred to fresh pre-heated buffer solutions to maintain sink conditions and the samples analysed by UV/Vis spectroscopy. Respective masses of drug released were determined using absorbance values at 292 nm in conjugation with freshly prepared calibration solutions, as previously described (Irwin, et al. 2013). Following completion of the release experiment, remaining ofloxacin was released by immersing finely divided samples in fresh buffer solutions and shaking at 37°C. The mechanism of drug release from the polymers was determined by fitting data to the generalized power model:

$$F = K_{KP}t^n$$

where F represents the fractional drug release in time t, K_{KP} is a rate constant incorporating geometric and structural characteristics of the release system and n is the release exponent used to characterize the mechanism of release (Korsmeyer, et al. 1983; Peppas 1985).

2.3. Statistics

All experiments were carried out using at least three replicates and results are expressed as mean ± standard deviation. Statistical analysis was performed with Analysis of Variance (ANOVA) software. Post hoc comparisons of individual mean values were performed by the Tukey-Kramer test, with a p value <0.05 denoting significance.

3. Results and discussion

Polymerisable derivatives of Poloxamer 188 were prepared *via* esterification of the terminal hydroxyl groups of the poloxamer moieties with methacryloyl chloride. By employing a large excess of Poloxamer 188 to methacryloyl chloride, esterification at only one terminal position was achieved, as shown in Scheme 1.

Alternatively, esterification at both terminal positions was achieved by employment of a 2:1 stoichiometric ratio of the methacryloyl chloride and poloxamer reactants, as shown in Scheme 2.

3.1. Leaching of non-methacrylated poloxamer (NMP) from p(MMP-*co*-HEMA) copolymers

The fraction of NMP released from the p(MMP-*co*-HEMA) copolymers during the rinsing step is shown in Figure 1.

This graph illustrates that as the theoretical mass of poloxamer within the matrix increased, longer periods of time were required for the maximum levels of NMP to leach out of the systems (approximately 1.5 h, 2.5 h and 3.5 h for the 1%, 5% and 10% MMP-containing copolymers respectively). In all cases, however, significant fractions of NMP remained within the matrices despite prolonged periods of soaking. The p(MMP-*co*-HEMA) copolymers with weight ratios of 1%, 5% and 10% MMP relative to the HEMA content retained 69%, 32% and 47% of the loaded NMP within their matrices respectively. This retention phenomenon was attributed to a combination of molecular entanglements and micellar aggregation of the NMP moieties with other NMP molecules and covalently-attached MMP moieties (Matanovic, et al. 2015).

3.2. Equilibrium water content

Equilibrium water contents (EWCs) of the MMP- and DMP-containing copolymers, NMP-loaded p(HEMA)) and the p(HEMA) control are shown in Table 3.

Table 3: EWCs of the synthesized polymers

Polymer	EWC (%) (Mean ± S.D.)
p(HEMA)	58.5 ± 3.85
NMP-loaded p(HEMA)	126.36 ± 1.03
1% p(MMP-*co*-HEMA)	96.21 ± 2.49
5% p(MMP-*co*-HEMA)	123.73 ± 2.24
10% p(MMP-*co*-HEMA)	227.44 ± 2.84
1% p(DMP-*co*-HEMA)	65.1 ± 0.94
5% p(DMP-*co*-HEMA)	75.82 ± 1.05
10% p(DMP-*co*-HEMA)	87.23 ± 1.74

With the ability to swell and retain significant amounts of water within their networks, all the novel copolymers can be classed as hydrogels (Ahmed 2015). Statistical differences were observed in the EWCs between all synthesized polymers, with the exception of 5% p(MMP-*co*-HEMA) and NMP-loaded p(HEMA). The latter was synthesized to contain the same amount of NMP as that remaining within the matrix of 5% p(MMP-*co*-HEMA) following leaching of the non-methacrylated moiety during the rinsing step. These results therefore highlight a dependency of the EWC on the quantity of unmodified poloxamer retained within the polymer matrix. The significantly higher EWCs of the MMP- and DMP-containing copolymers than the p(HEMA) control furthermore highlight the higher affinity for water uptake upon incorporation of methacrylated poloxamer within the p(HEMA) matrix, with the

EWCs increasing as the percentage of methacylated poloxamer within their networks increased. Moreover, comparison of the EWCs between the MMP- and DMP-containing copolymers revealed significantly lower values for the latter polymers, as expected, due to the presence of NMP within the p(MMP-*co*-HEMA) copolymer matrices and the increased crosslink density of the p(DMP-*co*-HEMA) copolymers. DMP, with two terminal polymerizable groups, behaves as a crosslinker upon copolymerisation with 2-HEMA, restricting flexibility of the polymer chains and ultimately reducing the capacity for water uptake (Fu, et al. 2016).

3.3. Contact angle

The angle made by a droplet of liquid in contact with a solid surface provides a measure of surface water wettability (Grundke, et al. 2015). The advancing and receding dynamic contact angles, formed by expansion of a droplet over a previously unwetted surface and retraction of a droplet from a previously wetted surface respectively (do Nascimento, et al. 2016; Grundke, et al. 2015), of the MMP- and DMP-containing copolymers, NMP-loaded p(HEMA)) and the p(HEMA) control are shown in Table 4.

Table 4: Dynamic contact angles of the synthesized polymers

Polymer	Contact Angle (°) (Mean ± S.D.)	
	Advancing	Receding
p(HEMA)	91.3 ± 1.65	92.5 ± 1.35
NMP-loaded p(HEMA)	92.0 ± 0.700	93.0 ± 1.10
1% p(MMP-*co*-HEMA)	92.0 ± 2.20	93.0 ± 2.00
5% p(MMP-*co*-HEMA)	92.0 ± 0.800	93.3 ± 0.850
10% p(MMP-*co*-HEMA)	98.0 ± 3.75	98.1 ± 4.75
1% p(DMP-*co*-HEMA)	90.5 ± 1.15	92.3 ± 0.907
5% p(DMP-*co*-HEMA)	91.8 ± 0.451	93.4 ± 0.404
10% p(DMP-*co*-HEMA)	92.7 ± 1.25	94.1 ± 1.15

Copolymers containing a weight ratio of 10% MMP relative to the HEMA content displayed significantly higher advancing contact angles than all other materials. The increased contact angle indicates an increase in the hydrophobic character of the polymer, which is attributed to shielding of the hydrophilic moieties of the p(HEMA) hydrogel by comparatively more hydrophobic alkyl chains of the poloxamer moiety (Yuan and Lee 2013). Receding contact angles were similar between all synthesized polymers, with the exception of 10% p(MMP-*co*-HEMA) and 1% p(DMP-*co*-HEMA).

In addition, none of the examined polymers exhibited significant contact angle hysteresis as a result of restricted polymer chain mobility and subsequently hindered molecular reorientation of surface-localized functional groups during the immersion process (do Nascimento, et al. 2016; Grundke, et al. 2015).

3.4. Tensile analysis

The effect of copolymerization with MMP and DMP on mechanical properties of the polymers was herein investigated by determination of ultimate tensile strength and Young's modulus of elasticity, which respectively provide a measure of polymer brittleness and rigidity (Kianfar, et al. 2011). Values of ultimate tensile strength and Young's modulus for the synthesized polymers are shown in Table 5.

Table 5: Mechanical properties of the synthesized polymers

Polymer	Ultimate tensile strength ($x10^5$, Pa) (Mean ± S.D.)	Young's modulus of elasticity ($x10^5$, Pa) (Mean ± S.D.)
p(HEMA)	4.15 ± 1.18	9.89 ± 1.29
NMP-loaded p(HEMA)	2.80 ± 0.423	3.87 ± 0.094
1% p(MMP-*co*-HEMA)	4.32 ± 0.532	7.35 ± 0.872
5% p(MMP-*co*-HEMA)	2.91 ± 0.542	3.49 ± 0.426
10% p(MMP-*co*-HEMA)	1.39 ± 0.374	1.86 ± 0.195
1% p(DMP-*co*-HEMA)	4.78 ± 0.399	9.49 ± 0.445
5% p(DMP-*co*-HEMA)	4.57 ± 0.407	8.67 ± 0.361
10% p(DMP-*co*-HEMA)	8.81 ± 2.13	10.3 ± 0.511

No significant differences were observed in ultimate tensile strength between the synthesized polymers and the control p(HEMA), with the exception of the 10% MMP- and 10% DMP-containing copolymers, which displayed significantly lower and higher ultimate tensile strength than the p(HEMA) control respectively. Ultimate tensile strength of the 10% DMP-containing copolymers was, in addition,

significantly higher than all other synthesized polymers, whereas the 10% MMP-containing copolymers displayed statistically lower ultimate tensile strength than the materials copolymerized with DMP (1%, 5% and 10%) and 1% MMP.

With regards to the elastic moduli, values for all MMP-containing copolymers, NMP-loaded p(HEMA) and 5% p(DMP-*co*-HEMA) were significantly lower than for p(HEMA). Significant differences were also observed between NMP-loaded p(HEMA) and all copolymers, with the exception of 5% p(MMP-*co*-HEMA). Comparison of Young's moduli between the DMP- and MMP-containing copolymers revealed significantly higher values for the former materials.

When loaded into the p(HEMA) matrix during polymerization, poloxamer moieties effectively act as plasticisers and ultimately reduce ultimate tensile strength and elastic modulus through disruption of the polymer network and distension of the polymer chains (Cavallari, et al. 2013). In contrast, the significant increase in ultimate tensile strength upon copolymerization with a 10% weight ratio of the dimethacrylated moiety was expected as a result of the increased crosslink density of the copolymer matrix in comparison to control p(HEMA). Crosslinking of the polymer matrix has previously been investigated as a strategy for improving the mechanical properties of hydrogels which, as a result of their high water contents and corresponding lower tensile strengths, are often limited in application to surface modification of existing devices (Jones, et al. 2005; Low, et al. 2015; Sanchez-Ferrero, et al. 2015).

3.5. Calcium and magnesium encrustation

Urological devices are particularly susceptible to encrustation as a result of infection by urease-secreting urinary pathogens such as *Proteus mirabilis* (Stickler and Feneley

2010). The consequential elevation of urine pH leads to precipitation of crystals of magnesium ammonium phosphate (struvite) and calcium phosphate (hydroxyapatite) in the urine (Stickler and Morgan 2006). Continued surface encrustation can ultimately obstruct the catheter lumen leading to urinary retention and further clinical complications such as pyelonephritis and septicemia (Stickler 2014). Surface densities of encrusting calcium and magnesium deposits on all synthesized polymers following a one-week period of suspension in artificial urine are shown in Table 6.

Table 6: Calcium and magnesium encrustation on synthesized polymer surfaces

Polymer	Calcium encrustation (surface density, μgcm^{-2}) (Mean ± S.D.)	Magnesium encrustation (surface density, μgcm^{-2}) (Mean ± S.D.)
p(HEMA)	0.069 ± 0.0026	0.024 ± 0.0002
NMP-loaded p(HEMA)	0.051 ± 0.0046	0.021 ± 0.0030
1% p(MMP-*co*-HEMA)	0.036 ± 0.0042	0.017 ± 0.0020
5% p(MMP-*co*-HEMA)	0.014 ± 0.0020	0.009 ± 0.0010
10% p(MMP-*co*-HEMA)	0.009 ± 0.0040	0.002 ± 0.0010
1% p(DMP-*co*-HEMA)	0.043 ± 0.0036	0.023 ± 0.0010
5% p(DMP-*co*-HEMA)	0.021 ± 0.0030	0.019 ± 0.0020
10% p(DMP-*co*-HEMA)	0.012 ± 0.0020	0.016 ± 0.0020

Loading of NMP and copolymerization with the MMP and DMP moieties were found to significantly reduce the level of calcium encrustation with respect to the control p(HEMA) surface, with reductions of up to 87% reported for the 10% MMP-

containing copolymers. Statistically-reduced magnesium encrustation was also demonstrated on all copolymer surfaces relative to control p(HEMA), with the exception of the 1% and 5% DMP-containing copolymers. For example, the surface density of magnesium deposits was approximately 92% lower on 10% p(MMP-*co*-HEMA) than on p(HEMA). Furthermore, while surfaces densities of calcium encrustation were observed to decrease as the weight percentage of methacrylated poloxamer increased, statistical analysis revealed levels of encrustation were similar between the MMP- and DMP-containing copolymers at each percentage loading.

3.6. Bacterial adherence

Bacterial resistance of the synthesized copolymers was herein examined by challenging the novel materials over a 4 h incubation period with clinical isolates of *E. coli*. Adherence of this clinical strain to the synthesized polymers relative to the p(HEMA) control is reported in Table 7.

Table 7: Adherence of *E. coli* to the synthesized polymers

Polymer	Adherence of *E. coli* relative to p(HEMA) control (%) (Mean ± S.D.)
p(HEMA)	100 ± 3.72
NMP-loaded p(HEMA)	24.6 ± 17.9
1% p(MMP-*co*-HEMA)	18.4 ± 8.04
5% p(MMP-*co*-HEMA)	9.96 ± 5.88
10% p(MMP-*co*-HEMA)	8.64 ± 1.44
1% p(DMP-*co*-HEMA)	75.3 ± 3.48
5% p(DMP-*co*-HEMA)	53.7 ± 1.08
10% p(DMP-*co*-HEMA)	46.0 ± 0.240

Copolymerization with the methacrylated poloxamers was demonstrated to be an efficacious strategy to reduce fouling by this common urinary pathogen relative to a commonly used hydrogel, p(HEMA), which itself has been demonstrated to give significant reductions in bacterial adherence in comparison with other medical device polymers, including silicone (Kodjikian, et al. 2002). All copolymers displayed statistically lower bacterial adherence relative to control p(HEMA), with reductions in excess of 90% reported for 5% and 10% p(MMP-*co*-HEMA).

The observed resistance to encrustation and bacterial adherence of the MMP- and DMP-containing copolymers in comparison to the p(HEMA) control was attributed to surface protrusion of the hydrophilic PEO chains of the poloxamer moieties. Furthermore, the reduced susceptibility to bacterial adherence, and significantly increased resistance to magnesium encrustation, of the MMP-containing copolymers in comparison to their DMP-containing counterparts was expected on account of the

presence of mobile chains of NMP in combination with the higher mobility of the PEO chains of the monomethacrylated species following copolymerization in comparison to the dimethacylated moieties, which are mostly crosslinked within the copolymer matrix. This phenomenon, known as steric stabilization, has been widely reported for surface-tethered poly(ethylene glycol) chains, in which their conformational flexibility and large exclusion volume have been demonstrated to prevent macromolecular and cellular surface adhesion (Otsuka, et al. 2001).

3.7. Drug release

In addition to their non-fouling properties, the hydrophobic cores of surface-tethered micellar structures have been investigated for their ability to function as reservoirs from which controlled release of hydrophobic drugs can proceed (Otsuka, et al. 2001). With infection rates of up to 100% reported for urinary catheters without antibiotic coverage, and hospital stays prolonged by up to 25 days, efficacious strategies to prevent device-associated infections are urgently needed (Riley, et al. 1995). We herein investigated the ability of the synthesized copolymers to control release of the fluoroquinolone antibiotic, ofloxacin, following loading in a saturated drug solution. Plots of drug release with time into 1% w/v benzalkonium solutions are shown in Figures 2 and 3.

Copolymerization with MMP in weight ratios of 5% and 10% relative to the HEMA content and physical loading of NMP were found to significantly increase the rate of ofloxacin release in comparison to the p(HEMA) control, 1% p(MMP-*co*-HEMA) and the DMP-containing copolymers, as displayed in Figures 2 and 3. Respective release from p(MMP-*co*-HEMA) copolymers with a 1%, 5% and 10% weight ratio of MMP after 1 h approximated 31%, 74% and 85% respectively. In comparison to their

MMP-containing counterparts, release rates from the p(DMP-*co*-HEMA) copolymers were similar to p(HEMA) and release was sustained over significantly longer periods of time. Respective release from copolymers containing a weight ratio of 1%, 5% and 10% DMP after 1 h approximated 24%, 26% and 36% respectively. Rates of water uptake, and resultant drug release, from hydrogels is a complex phenomenon governed by many factors including particle size, solubility and ionization state of the drug (Wen and Park 2010), pH and ionic strength of the release medium, and polymer characteristics including crosslink density, chemical composition, presence of ionisable functional groups and hydrophilicity, which in turn determine the resultant degree of swelling, pore interconnections and interactions with the diffusing drug (Hoffman 2002; Luo, et al. 2009; Sailaja, et al. 2011). As expected, the behavior observed herein, namely the significantly faster rates of hydrophobic drug release from the 5% and 10% p(MMP-*co*-HEMA) copolymers and the NMP-loaded p(HEMA) in contrast to the more sustained release from p(HEMA), 1% p(MMP-*co*-HEMA) and their p(DMP-*co*-HEMA) counterparts was analogous to that observed in the equilibrium swelling study, where the former three polymers displayed EWCs >100% and the latter polymers displayed EWCs <100%. The rapid drug release from the polymers containing long chain NMP moieties was again attributed to their greater flexibility and expanded polymeric networks in contrast to the increased crosslink density and consequential higher rigidity of the p(DMP-*co*-HEMA) matrices. Significantly lower burst and overall rates of release from crosslinked polymers in comparison to uncrosslinked controls has been widely reported (Martinez, et al. 2014; Zhong, et al. 2015).

Release exponents, n, which are indicative of the mechanism of release, were determined for all polymers by fitting release data to the power law model, $F = K_{KP}t^n$,

and are reported in Table 8 (Peppas 1985).

Table 8: Release exponents for ofloxacin release from the synthesized polymers

Polymer	Release exponent *n* (Mean ± S.D.)
p(HEMA)	0.32 ± 0.01
NMP-loaded p(HEMA)	0.41 ± 0.01
1% p(MMP-*co*-HEMA)	0.41 ± 0.01
5% p(MMP-*co*-HEMA)	0.41 ± 0.01
10% p(MMP-*co*-HEMA)	0.39 ± 0.02
1% p(DMP-*co*-HEMA)	0.39 ± 0.02
5% p(DMP-*co*-HEMA)	0.43 ± 0.01
10% p(DMP-*co*-HEMA)	0.41 ± 0.04

In all cases, release exponents were <0.5. This deviation from the diffusional model of release ($n = 0.5$), which is characteristic of drug release from hydrated polymer matrices, may be attributed to further swelling of, and potential channel formation throughout, the polymer matrices as a result of the presence of the long alkyl chains of the poloxamer moiety in combination with interactions with the cationic surfactant benzalkonium chloride, which was added to the release medium to increase solubility of the hydrophobic quinolone, ofloxacin (Ivanova, et al. 2001)

4. Conclusions

There remains an urgent and unmet need for efficacious strategies to prevent the escalating global healthcare burden of catheter-associated infections. As reported

herein, a combinatorial approach, namely active agent incorporation and surface modification, holds significant potential to achieve this goal. Copolymerization of p(HEMA) with methacrylated Poloxamer 188 in a weight ratio of 10% relative to the HEMA content reduced surface adherence of *E. coli* and encrusting crystalline deposits by more than 90% relative to control p(HEMA). Furthermore, these systems provide the additional benefit of facile tailoring of the kinetics of hydrophobic drug release depending on the resultant application through ready manipulation of the extent of poloxamer methacrylation and incorporation within the copolymer. Faster release of loaded hydrophobic drug, at rates up to 16-fold higher than that from p(HEMA), was achieved from polymers containing NMP, whereas more sustained released over a period of up to four days was observed from the more highly crosslinked p(DMP-*co*-HEMA) matrices.

Acknowledgements

This work was supported by the Department of Employment and Learning (now Department for the Economy) Northern Ireland.

References

Ahmed, E.M., 2015. Hydrogel: Preparation, characterization, and applications: A review. Journal of Advanced Research, 6, 105-121. doi: 10.1016/j.jare.2013.07.006.

Cavallari, C., Fini, A., Ospitali, F., 2013. Mucoadhesive multiparticulate patch for the intrabuccal controlled delivery of lidocaine. European Journal of Pharmaceutics and Biopharmaceutics, 83, 405-414. doi: 10.1016/j.ejpb.2012.10.004.

Cloutier, M., Mantovani, D., Rosei, F., 2015. Antibacterial coatings: challenges, perspectives, and opportunities. Trends Biotechnol., 33, 637-652. doi: 10.1016/j.tibtech.2015.09.002.

Coad, B.R., Griesser, H.J., Peleg, A.Y., Traven, A., 2016. Anti-infective surface coatings: design and therapeutic promise against device-associated infections. Plos Pathogens, 12, e1005598. doi: 10.1371/journal.ppat.1005598.

Daniels, K.R., Lee, G.C., Frei, C.R., 2014. Trends in catheter-associated urinary tract infections among a national cohort of hospitalized adults, 2001-2010. Am. J. Infect. Control, 42, 17-22. doi: 10.1016/j.ajic.2013.06.026.

do Nascimento, R.M., Cottin-Bizonne, C., Pirat, C., Ramos, S.M.M., 2016. Water drop evaporation on mushroom-like superhydrophobic surfaces: temperature effects. Langmuir, 32, 2005-2009. doi: 10.1021/acs.langmuir.5b04445.

Fisher, L.E., Hook, A.L., Ashraf, W., Yousef, A., Barrett, D.A., Scurr, D.J., Chen, X., Smith, E.F., Fay, M., Parmenter, C.D.J., Parkinson, R., Bayston, R., 2015. Biomaterial modification of urinary catheters with antimicrobials to give long-term broadspectrum antibiofilm activity. J. Controlled Release, 202, 57-64. doi: 10.1016/j.jconrel.2015.01.037.

Francolini, I., Donelli, G., Vuotto, C., Baroncini, F.A., Stoodley, P., Taresco, V., Martinelli, A., D'Ilario, L., Piozzi, A., 2014. Antifouling polyurethanes to fight device-related staphylococcal infections: synthesis, characterization, and antibiofilm efficacy. Pathogens and Disease, 70, 401-407. doi: 10.1111/2049-632X.12155.

Fu, L., Cao, T., Lei, Z., Chen, H., Shi, Y., Xu, C., 2016. Superabsorbent nanocomposite based on methyl acrylic acid-modified bentonite and sodium polyacrylate: Fabrication, structure and water uptake. Mater Des, 94, 322-329. doi: 10.1016/j.matdes.2016.01.014.

Gilmore, B.F., Carson, L., 2015. Bioactive biomaterials for controlling biofilms, in: Barnes, L., Cooper, I.R. (Eds.), Biomaterials and Medical Device-Associated Infections, Woodhead Publishing, Cambridge, UK, pp. 163-184.

Greene, M.T., Fakih, M.G., Fowler, K.E., Meddings, J., Ratz, D., Safdar, N., Olmsted, R.N., Saint, S., 2014. Regional variation in urinary catheter use and catheter-associated urinary tract infection: results from a National Collaborative. Infection Control and Hospital Epidemiology, 35, S99-S106. doi: 10.1086/677825.

Grundke, K., Poeschel, K., Synytska, A., Frenzel, R., Drechsler, A., Nitschke, M., Cordeiro, A.L., Uhlmann, P., Welzel, P.B., 2015. Experimental studies of contact angle hysteresis phenomena on polymer surfaces - Toward the understanding and control of wettability for different applications. Adv. Colloid Interface Sci., 222, 350-376. doi: 10.1016/j.cis.2014.10.012.

Gultekinoglu, M., Sarisozen, Y.T., Erdogdu, C., Sagiroglu, M., Aksoy, E.A., Oh, Y.J., Hinterdorfer, P., Ulubayram, K., 2015. Designing of dynamic polyethyleneimine (PEI) brushes on polyurethane (PU) ureteral stents to prevent infections. Acta Biomaterialia, 21, 44-54. doi: 10.1016/j.actbio.2015.03.037.

Hoffman, A.S., 2002. Hydrogels for biomedical applications. Adv. Drug Deliv. Rev., 54, 3-12. doi: 10.1016/s0169-409x(01)00239-3.

Irwin, N.J., McCoy, C.P., Jones, D.S., Gorman, S.P., 2013. Infection-responsive drug delivery from urinary biomaterials controlled by a novel kinetic and thermodynamic approach. Pharm. Res., 30, 857-865. doi: 10.1007/s11095-012-0927-x.

Ivanova, R., Alexandridis, P., Lindman, B., 2001. Interaction of poloxamer block copolymers with cosolvents and surfactants. Colloids and Surfaces A-Physicochemical and Engineering Aspects, 183, 41-53. doi: 10.1016/S0927-7757(01)00538-6.

Jamal, M.A., Hachem, R.Y., Rosenblatt, J., McArthur, M.J., Felix, E., Jiang, Y., Tailor, R.C., Raad, I., 2015. In vivo biocompatibility and in vitro efficacy of antimicrobial gendine-coated central catheters. Antimicrob. Agents Chemother., 59, 5611-5618. doi: 10.1128/AAC.00834-15.

Jones, D., Djokic, J., McCoy, C., Gorman, S., 2002. Poly(epsilon-caprolactone) and poly(epsilon-caprolactone)-polyvinylpyrrolidone-iodine blends as ureteral biomaterials: characterisation of mechanical and surface properties, degradation and resistance to encrustation in vitro. Biomaterials, 23, 4449-4458. doi: 10.1016/S0142-9612(02)00158-8.

Jones, D., McLaughlin, D., McCoy, C., Gorman, S., 2005. Physicochemical characterisation and biological evaluation of hydrogel-poly(epsilon-caprolactone) interpenetrating polymer networks as novel urinary biomaterials. Biomaterials, 26, 1761-1770. doi: 10.1016/j.biomaterials.2004.06.002.

Kaizu, K., Alexandridis, P., 2015. Micellization of polyoxyethylene-polyoxypropylene block copolymers in aqueous polyol solutions. Journal of Molecular Liquids, 210, 20-28. doi: 10.1016/j.molliq.2015.04.039.

Keane, P., Bonner, M., Johnston, S., Zafar, A., Gorman, S., 1994. Characterization of Biofilm and Encrustation on Ureteral Stents In-Vivo. Br. J. Urol., 73, 687-691. doi: 10.1111/j.1464-410X.1994.tb07557.x.

Kianfar, F., Antonijevic, M.D., Chowdhry, B.Z., Boaten, J.S., 2011. Formulation development of a carrageenan based delivery system for buccal drug delivery using ibuprofen as a model drug. Journal of Biomaterials and Nanobiotechnology, 2, 582-595.

Kodjikian, L., Burillon, C., Chanloy, C., Bostvironnois, V., Pellon, G., Mari, E., Freney, J., Roger, T., 2002. In vivo study of bacterial adhesion to five types of intraocular lenses. Investigative Ophthalmology and Visual Science, 43, 3717-3721.

Korsmeyer, R.W., Gurny, R., Doelker, E., Buri, P., Peppas, N.A., 1983. Mechanisms of solute release from porous hydrophilic polymers. Int. J. Pharm., 15, 25-35. doi: 10.1016/0378-5173(83)90064-9.

Li, A., Zhang, D., 2016. Synthesis and characterization of cleavable core-cross-linked micelles based on amphiphilic block copolypeptoids as smart drug carriers. Biomacromolecules, 17, 852-861. doi: 10.1021/acs.biomac.5b01561.

Li, J., Guo, S., Wang, M., Ye, L., Yao, F., 2015. Poly(lactic acid)/poly(ethylene glycol) block copolymer based shell or core cross-linked micelles for controlled release of hydrophobic drug. Rsc Advances, 5, 19484-19492. doi: 10.1039/c4ra14376k.

Low, Z.W., Chee, P.L., Kai, D., Loh, X.J., 2015. The role of hydrogen bonding in alginate/poly(acrylamide-co-dimethylacrylamide) and alginate/poly(ethylene glycol)

methyl ether methacrylate-based tough hybrid hydrogels. Rsc Advances, 5, 57678-57685. doi: 10.1039/c5ra09926a.

Luo, Y., Zhang, K., Wei, Q., Liu, Z., Chen, Y., 2009. Poly(MAA-co-AN) hydrogels with improved mechanical properties for theophylline controlled delivery. Acta Biomaterialia, 5, 316-327. doi:10.1016/j.actbio.2008.07.013.

Martinez, A.W., Caves, J.M., Ravi, S., Li, W., Chaikof, E.L., 2014. Effects of crosslinking on the mechanical properties, drug release and cytocompatibility of protein polymers. Acta Biomaterialia, 10, 26-33. doi: 10.1016/j.actbio.2013.08.029.

Matanovic, M.R., Grabnar, I., Gosenca, M., Grabnar, P.A., 2015. Prolonged subcutaneous delivery of low molecular weight heparin based on thermoresponsive hydrogels with chitosan nanocomplexes: Design, in vitro evaluation, and cytotoxicity studies. Int. J. Pharm., 488, 127-135. doi: 10.1016/j.ijpharm.2015.04.063.

Miles, A.A., Misra, S.S., Irwin, J.O., 1938. The estimation of the bactericidal power of the blood. J. Hyg., 38, 732-749.

Movassaghian, S., Merkel, O.M., Torchilin, V.P., 2015. Applications of polymer micelles for imaging and drug delivery. Wiley Interdisciplinary Reviews-Nanomedicine and Nanobiotechnology, 7, 691-707. doi: 10.1002/wnan.1332.

Otsuka, H., Nagasaki, Y., Kataoka, K., 2001. Self-assembly of block copolymers. Materials Today, 4, 30-36.

Peppas, N.A., 1985. Analysis of Fickian and non-Fickian drug release from polymers. Pharm. Acta Helv., 60, 110-111.

Riley, D., Classen, D., Stevens, L., Burke, J., 1995. A large randomized clinical-trial of a silver-impregnated urinary catheter - lack of efficacy and staphylococcal superinfection. Am. J. Med., 98, 349-356. doi: 10.1016/S0002-9343(99)80313-1.

Rodriguez-Emmenegger, C., Janel, S., de los Santos Pereira, A., Bruns, M., Lafont, F., 2015. Quantifying bacterial adhesion on antifouling polymer brushes via single-cell force spectroscopy. Polymer Chemistry, 6, 5740-5751. doi: 10.1039/c5py00197h.

Sailaja, G.S., Ramesh, P., Varma, H., 2011. Effect of surface functionalization on the physicochemical properties of a novel biofunctional copolymer. J. Appl. Polym, Sci., 121, 3509-3515. doi: 10.1002/app.34157.

Sanchez-Ferrero, A., Mata, A., Mateos-Timoneda, M.A., Rodriguez-Cabello, J.C., Alonso, M., Planell, J., Engel, E., 2015. Development of tailored and self-mineralizing citric acid-crosslinked hydrogels for in situ bone regeneration. Biomaterials, 68, 42-53. doi: 10.1016/j.biomaterials.2015.07.062.

Stickler, D.J., 2014. Clinical complications of urinary catheters caused by crystalline biofilms: something needs to be done. J. Intern. Med., 276, 120-129. doi: 10.1111/joim.12220.

Stickler, D.J., Feneley, R.C., 2010. The encrustation and blockage of long-term indwelling bladder catheters: a way forward in prevention and control. Spinal Cord, 48, 784-790. doi: 10.1038/sc.2010.32.

Stickler, D.J., Morgan, S.D., 2006. Modulation of crystalline *Proteus mirabilis* biofilm development on urinary catheters. J. Med. Microbiol., 55, 489-494.

Tunney, M.M., Bonner, M.C., Keane, P.F., Gorman, S.P., 1996. Development of a model for assessment of biomaterial encrustation in the upper urinary tract. Biomaterials, 17, 1025-1029.

Tunney, M.M., Gorman, S.P., 2002. Evaluation of a poly(vinyl pyrollidone)-coated biomaterial for urological use. Biomaterials, 23, 4601-4608. doi: 10.1016/S0142-9612(02)00206-5.

Wang, R., Neoh, K.G., Kang, E., Tambyah, P.A., Chiong, E., 2015. Antifouling coating with controllable and sustained silver release for long-term inhibition of infection and encrustation in urinary catheters. Journal of Biomedical Materials Research Part B-Applied Biomaterials, 103, 519-528. doi: 10.1002/jbm.b.33230.

Wei, Q., Becherer, T., Noeske, P.M., Grunwald, I., Haag, R., 2014. A universal approach to crosslinked hierarchical polymer multilayers as stable and highly effective antifouling coatings. Adv Mater, 26, 2688-2693. doi: 10.1002/adma.201304737.

Wen, H., Park, K., 2010. Introduction and overview of oral controlled release formulation design, in: Wen, H., Park, K. (Eds.), Oral Controlled Release Formulation Design and Drug Delivery. Theory to Practice. John Wiley and Sons Inc., New Jersey, pp. 5-8.

Yuan, Y., Lee, R., 2013. Contact angle and wetting properties, in: Bracco, G., Holst, B. (Eds.), Surface Science Techniques, Springer, Berlin, pp. 3-34.

Zeng, N., Dumortier, G., Maury, M., Mignet, N., Boudy, V., 2014. Influence of additives on a thermosensitive hydrogel for buccal delivery of salbutamol: Relation

between micellization, gelation, mechanic and release properties. Int. J. Pharm., 467, 70-83. doi: 10.1016/j.ijpharm.2014.03.055.

Zhong, Y., Zhang, J., Cheng, R., Deng, C., Meng, F., Xie, F., Zhong, Z., 2015. Reversibly crosslinked hyaluronic acid nanoparticles for active targeting and intelligent delivery of doxorubicin to drug resistant CD44+ human breast tumour xenografts. J. Control. Release, 205, 144-154. doi: 10.1016/j.jconrel.2015.01.012.

Figure Captions

Scheme 1: Monomethacrylation of Poloxamer 188.

Scheme 2: Dimethacrylation of Poloxamer 188.

Figure 1: Release of NMP from the MMP-containing copolymers during the rinsing step.

Figure 2: Release of ofloxacin from NMP-loaded p(HEMA) and copolymers containing 5% and 10% MMP.

Figure 3: Release of ofloxacin from p(HEMA), 1% p(MMP-co-HEMA) and the DMP-containing copolymers.

Figure 1.

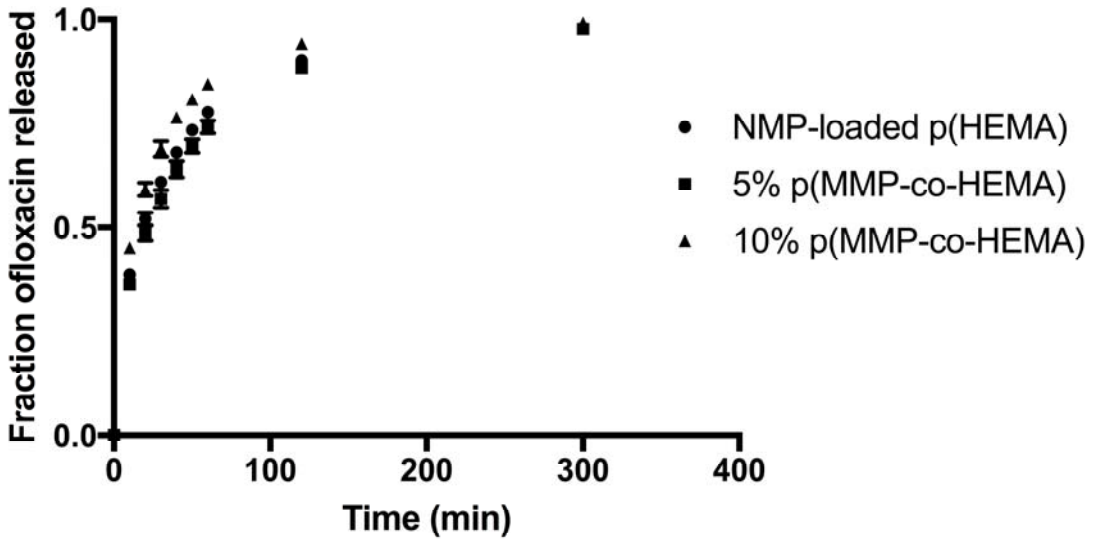

Figure 2.

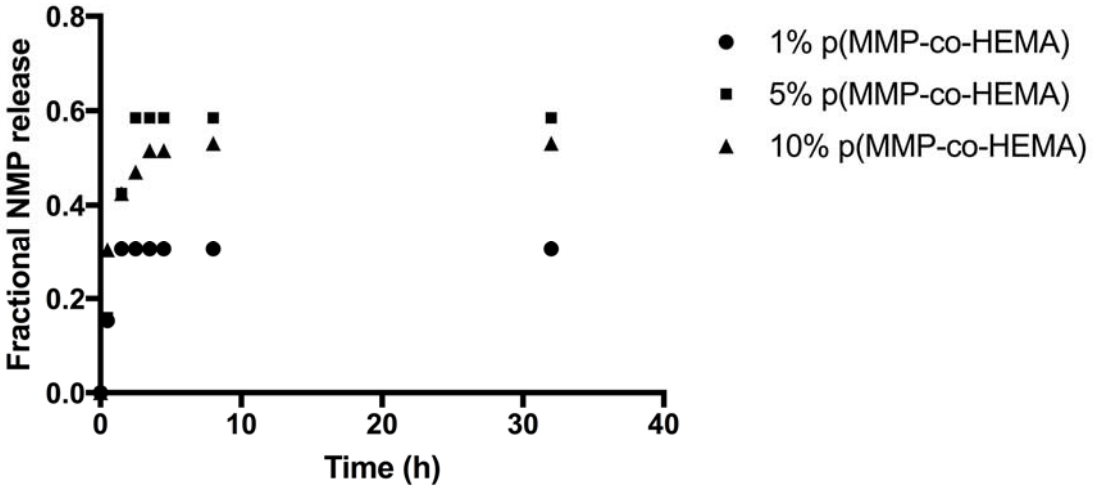

Figure 3.

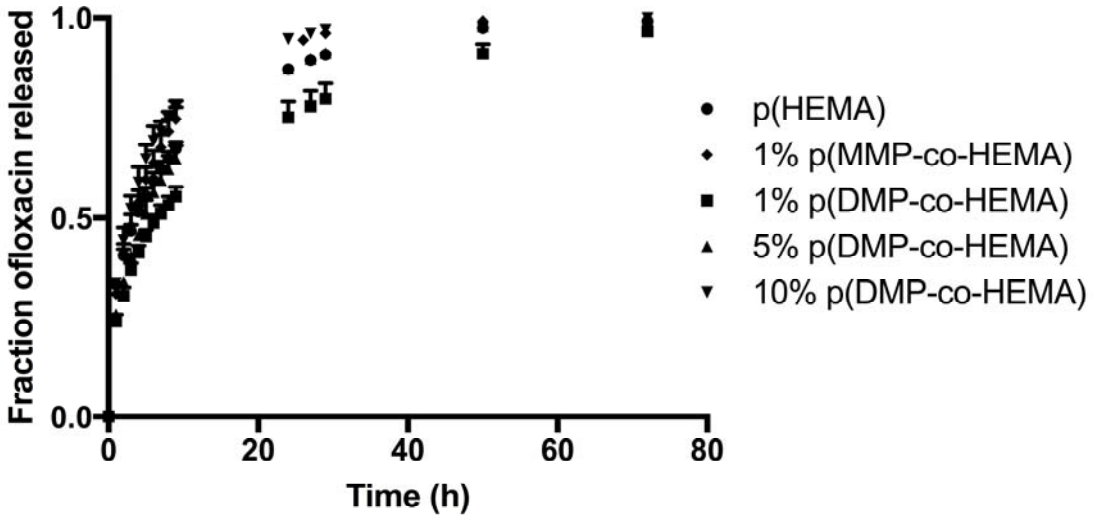
Fraction ofloxacin released
1.0
0.5
0.0
0
20
40
60
80
Time (h)
p(HEMA)
1% p(MMP-co-HEMA)
1% p(DMP-co-HEMA)
5% p(DMP-co-HEMA)
10% p(DMP-co-HEMA)

Scheme 1.

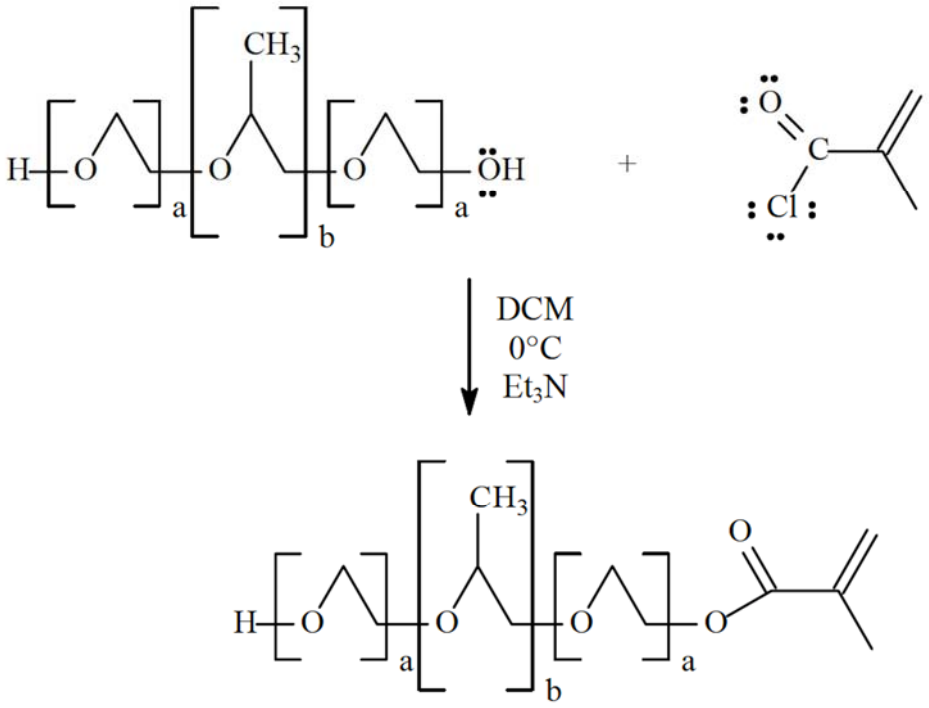

Scheme 2

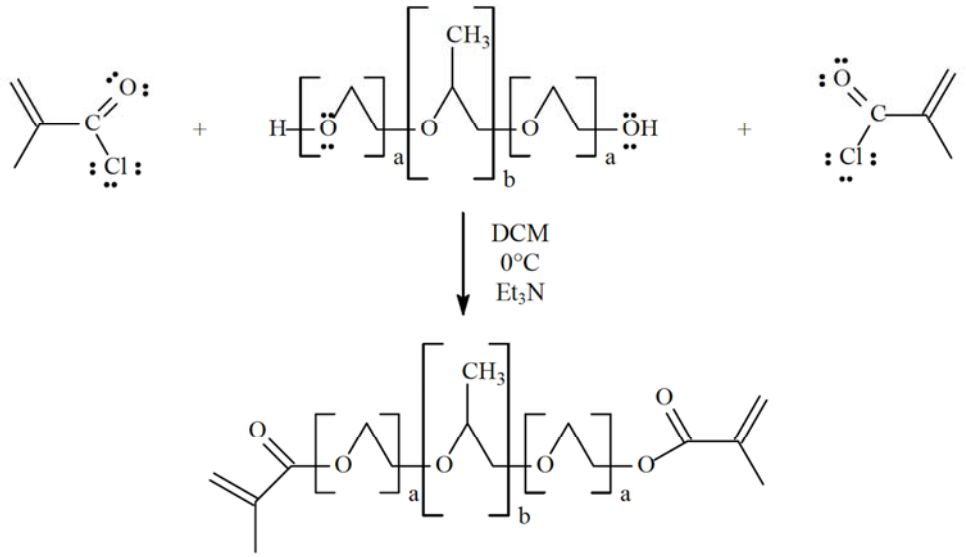
CH3
DCM
0°C
Et3N